Brain-wide projection reconstruction of single functionally defined neurons

Xiaowei Chen (xiaowei_chen@tmmu.edu.cn)
Third Military Medical University https://orcid.org/0000-0003-0906-6666

Meng Wang
Third Military Medical University

Ke Liu
Third Military Medical University

Jialin Li
Chongqing University

Junxia Pan
Third Military Medical University

Yongsheng Zhang
Huazhong University of Science and Technology

Longhui Li
Chongqing University

Wenyan Guo
Huazhong University of Science and Technology

Qianqian Xin
Third Military Medical University

Zhikai Zhao
Third Military Medical University

Yurong Liu
Huazhong University of Science and Technology

Zhenqiao Zhou
Brain Research Instrument Innovation Center, Suzhou Institute of Biomedical Engineering and Technology, Chinese Academy of Sciences https://orcid.org/0000-0001-9022-7644

Ting Zheng
Wuhan OE-Bio Co., Ltd, Wuhan 430074, China. Correspondence to: 1037 Luoyu Road, Wuhan 430074, China.

Yunyun Han
Huazhong University of Science & Technology

Chunqing Zhang
Third Military Medical University

Xiang Liao

Chongqing University

Shaoqun Zeng

Huazhong University of Science & Technology

Hongbo Jia

Suzhou Institute of Biomedical Engineering and Technology, Chinese Academy of Sciences
https://orcid.org/0000-0003-1585-2161

Article

Keywords: Axonal Projections, Information Flow, Physiological Functions, Plasmid Electroporation, Sound-evoked Response Map

Posted Date: March 1st, 2021

DOI: https://doi.org/10.21203/rs.3.rs-195997/v1

Version of Record: A version of this preprint was published at Nature Communications on March 22nd, 2022. See the published version at https://doi.org/10.1038/s41467-022-29229-0.

Abstract

Reconstructing axonal projections of single neurons at whole-brain level is a currently converging goal of the neuroscience community, which is fundamental to understanding the logic of information flow in the brain. Thousands of single neurons from different brain regions recently have been morphologically reconstructed, but the corresponding physiological functions of these reconstructed neurons are lacking. By combining two-photon Ca^{2+} imaging with targeted single-cell plasmid electroporation, we reconstructed the brain-wide morphologies of single neurons that were defined by a sound-evoked response map in the auditory cortex of awake mice. Long-range interhemispheric projections can be reliably labelled with co-injection of adeno-associated virus. This method avoids the randomness and ambiguity of conventional methods of neuronal morphological reconstruction, offering an avenue for developing a precise one-to-one map of neuronal projection and physiological function. Our method can be readily implemented in many laboratories that have been equipped with a standard two-photon microscope and electrophysiological devices.

Main Text

Understanding how neuronal functions are related to morphology is a central goal of modern neuroscience. Axonal projections determine how neurons route their physiological functional output information to target brain regions. However, even within a small brain region, neurons often exhibit extraordinary functional diversity and are spatially intermingled. Thus, there is a great demand for axonal projection reconstructions of neurons that are defined by physiological functions in a given brain region; three levels of methods are in principle available for this purpose. The first-level methods provide nonspecific labelling of neurons by expressing fluorescent proteins[1-3] for visualization and reconstruction using whole-brain serial sectioning imaging techniques[4-6]. At this level, the neurons to be labelled are usually randomly selected from a defined brain region. The second-level methods label neurons with fluorescent proteins based on specific molecular markers through a Cre-dependent expression procedure to enable the reconstruction of molecularly defined neuronal types[7]. Although highly relevant, molecularly defined cell types do not unambiguously define specific physiological functions under *in vivo* conditions. The third-level methods involve both electrophysiological recording and plasmid delivery to express fluorescent proteins *in vivo* by using a patch pipette on the same neurons[8,9]. These methods offer direct matching of single-cell physiological functions and axonal projections, but with the same caveat that chance largely determines which exact neurons are reconstructed. In addition, these methods have not yet yielded a complete reconstruction of neuronal morphology at the whole-brain level.

With the help of either recently developed high-throughput techniques[3,10] or extensive human labor[11], it may someday become possible for neurons with different types of physiological functions to be sufficiently sampled and reconstructed. However, neurons with specific response patterns such as those related to learning, memory and behaviour are sparse, constituting only a few percent of neurons in the relevant brain regions[12,13], which raises concerns that high-throughput techniques may yield highly

ambiguous results. Thus, there is a high but unmet demand for a method that enables precisely targeted labelling of neurons whose physiological functions have been defined *in vivo*. Here, we report a method that seamlessly combines two-photon Ca^{2+} imaging of cortical neuronal populations in awake mice[13,14] and post-mortem whole-brain serial sectioning imaging of dendrites and axonal projections using the technique of fluorescence micro-optical sectioning tomography (fMOST)[15]. As an example, we identified single neurons with specific tone-tuning response profiles[16] in the auditory cortex of awake mice and electroporated these neurons one by one to label their dendrites and axons. With the control of retrograde labelling[2] from the distant projection target area, we confirmed that long-range interhemispheric cortico-cortical projections can be reliably labelled by our method. Importantly, our method can be readily implemented in a broad range of laboratories that have been equipped with a standard two-photon microscope and conventional electrophysiological devices.

Briefly, our method consists of four key steps to achieve brain-wide reconstruction of functionally defined neurons in the mouse brain. Herein, as an example, we describe these steps for reconstructing targeted auditory cortical neurons with defined tone-tuning response properties (Fig. 1a and Supplementary Video 1): (1) A bulk population of the neurons located in layer 2/3 (L2/3) of the primary auditory cortex (A1) of awake mice was labelled by local injection of a Ca^{2+} fluorescent indicator dye, Cal-520 AM. Sound-evoked Ca^{2+} transients were recorded by two-photon Ca^{2+} imaging, and the frequency response area (FRA) and best frequency (BF) of each neuron were determined[16]. (2) Single neurons with specific tone-tuning properties of interest (in the example of Fig. 1, with BF = 16.3 kHz) were chosen to be targeted for the expression of a Cre-GFP (hSyn-eGFP-P2A-Cre-pA; for details, see Methods) plasmid by single-cell electroporation[17]. In order to enhance fluorescent protein expression in long-range projection axons, an adeno-associated virus (AAV) that contained a Cre-dependent expression cassette encoding mGFP (membrane green fluorescent protein) (AAV-hSyn-DIO-mGFP) was injected lateral to the site of the electroporated neurons. (3) Thirty days after single-cell electroporation, the animals were perfused, their brains were removed and transferred to the fMOST imaging device, and a whole-brain serial sectioning imaging dataset was acquired at submicron voxel resolution. (4) Morphological reconstruction and quantitative analysis were performed to study the axonal projection patterns of the imaged neurons.

Next, we illustrate step-by-step how and why we configured the relevant basic techniques to be combined, enabling complete and robust reconstruction of brain-wide projections of single functionally defined neurons. In the first step, we used a Ca^{2+} fluorescent indicator dye for two-photon neuronal population imaging in awake mice, recorded sound-evoked Ca^{2+} responses over multiple trials and then analysed the FRA and BF for individual neurons (Fig. 1b-d and Supplementary Fig. 1). We chose two example neurons (Fig. 1b, c) by the definition of BF = 16.3 kHz and targeted them for morphology labelling. A key point here is to perform acute functional imaging with synthetic Ca^{2+} dye that is gene free to avoid interference with the subsequent morphological labelling procedure, which relies on genetic approaches.

In the second step, to achieve complete fluorescent protein labelling of individual neurons, we combined two genetic approaches. First, a micropipette (electrical resistance of ~12 MΩ) containing intracellular

solution and a Cre-GFP plasmid was advanced towards the soma of each functionally defined target neuron one by one under live two-photon imaging guidance (Fig. 1e), by which electrical pulses (pulse amplitude -15 V, duration 500 μs per pulse, 100 pulses at 50 Hz per target cell) were applied to perforate the cellular membrane and deliver the plasmid into the cell body. Note that an intracellular Ca^{2+} dye, OGB-1 potassium salt, was also included in the micropipette solution to visualize the pipette and target neurons (Fig. 1e). Then, an AAV that contained a Cre-dependent expression cassette (double-floxed inverse open reading frame, DIO) encoding mGFP was injected into the extracellular space near the location of the electroporated neurons. We were able to monitor the expression level of GFP in the target neurons over days through *in vivo* two-photon imaging (Fig. 1f). Thirty days after electroporation, the expression of GFP reached a sufficiently high level for *post hoc* fMOST imaging. The key point in this step is the combination of single-cell plasmid electroporation and nearby local AAV injection to unlock robust fluorescence expression in target neurons. As such, the trouble of titrating the plasmid concentration for trading off between the expression level and cellular toxicity was bypassed. Moreover, the number of labelled neurons can be determined by the number of neurons electroporated (Supplementary Fig. 2).

In the third step, we performed whole-brain serial sectioning imaging at a resolution of 0.3 × 0.3 × 1 μm^3 (for details see Methods) with the fMOST technique (Supplementary Fig. 3). With our labelling technique from the second step, we were able to clearly identify the soma, dendrites and distant axons of each targeted neuron in the raw images (Supplementary Fig. 4). The complete morphology of each labelled neuron was reconstructed by manual tracing (Supplementary Fig. 5). For a trade-off between reconstruction accuracy and throughput, each neuron was traced by two experienced annotators, and the consensus result was approved (Supplementary Fig. 6)[18]. Then, all the reconstructed neurons were registered to the template of the Allen Brain Atlas, i.e., the Allen Mouse Common Coordinate Framework (CCF v3), combining the approaches of greyscale-based 3D registration and dense-landmark-based 2D registration in the local regions (Supplementary Fig. 7). In this step, we chose the fMOST imaging technique because of its relatively high z-resolution, which is ensured by mechanical sectioning and is important for resolving axons. In turn, the cost is that greater effort is required in the axon tracing procedure as well as brain map alignment with the standard Allen Framework.

In the last step, both the dendrites and the axonal projections of labelled neurons were completely traced, reconstructed and analysed (Fig. 2). In this example dataset consisting of two neurons from the same auditory cortex and with the same functional definition (BF = 16.3 kHz), we found that these two neurons exhibited distinct projection preferences (Fig. 2a, b). Neuron 1 projected extensively to bilateral hemispheres; its axons formed dense terminal fields at the contralateral target areas and mainly targeted the contralateral auditory cortex. In contrast, the projections from neuron 2 were mainly localized in regions including the ipsilateral striatum and auditory areas (Fig. 2c). We calculated the length and total number of branches for both axons and dendrites of the two neurons (Fig. 2c, d). Axonal length per area in the cerebral cortex has previously been reported to correlate strongly with the number of recipient neurons[19]. As shown in Fig. 2e, the length and total number of branches of axons were much larger for

neuron 1 than those for neuron 2, suggesting that neuron 1 may have more output recipients than neuron 2. In addition, the length and total number of branches of dendrites were also much larger for neuron 1 than those for neuron 2 (Fig. 2e), indicating that neuron 1 may receive more synaptic inputs than neuron 2.

We evaluated the axonal labelling quality achieved by our method through an independent set of experiments involving long-range retrograde labelling, which is an acknowledged standard in the community[2]. The long-range projection between bilateral auditory cortices was considered a challenging test metric because this contralateral cortico-cortical projection distance is 9.6 mm long, which is more than twice the ipsilateral cortico-striatal projection of 4.7 mm and is among the longest possible projections for L2/3 neurons in the mouse neocortex (Fig. 3a). First, we performed bulk retrograde labelling with AAV2/2-Retro expressing a red fluorescent protein (mRuby3) starting from L2/3 of the contralateral A1 (the injection site of AAV2/2-Retro-hSyn-H2B-mRuby3-WPRE-pA pointed by an arrow in the left auditory cortex in Fig. 3b), resulting in a fraction of neurons labelled in L2/3 of A1 on our single-neuron targeting side (the right auditory cortex in Fig. 3b). Then, by our method as described above involving both single-cell plasmid electroporation and local AAV injection, we electroporated a few neurons that were confirmed to possess such interhemispheric cortico-cortical projections (two neurons are targeted in Fig. 3c, d). Thirty days after electroporation, axonal terminals in the contralateral auditory cortex were clearly visible in all cases tested (Fig. 3e, f and Supplementary Fig. 8a, b; 9 neurons from 5 mice), indicating a 100% success rate in filling long-range axon collaterals by our method (see also Supplementary Video 2). In a parallel set of control experiments, we labelled L2/3 neurons in the A1 with confirmed interhemispheric cortico-cortical projections by single-cell electroporation of the Cre-GFP plasmid as described above, but with no combined nearby injection of AAV. For these control neurons, axonal projections could extend out of the local A1 but could not reach the confirmed destination of contralateral A1 (Fig. 3g, h and Supplementary Fig. 8c; 9 neurons from 5 mice), suggesting the importance of using the combined protocol for achieving robust long-range axon labelling.

In summary, we developed a novel method to enable the analysis of brain-wide axonal projection logic of single neurons that are functionally defined, advancing one level up towards the goal of precise understanding the principles of the brain structure and function at the single-neuron level. Two major advances of our method are as follows: (1) Precisely targeted labelling of single functionally defined neurons (Fig. 1 and 2). This is particularly useful for many brain regions whose neurons are functionally distinct and spatially intermingled. (2) Robust labelling of long-range axonal projections (Fig. 3). A bottleneck of our method is that the workflow involves multiple challenging techniques to be combined and intensive real-time interactive operations to be performed. However, once the method is well established and practised, a high success rate of > 90% can be achieved on a day-to-day basis. Moreover, our single-cell electroporation protocol can also use other plasmids in addition to those for morphological labelling, e.g., plasmids for optical manipulation of single neuronal functions[20]. Overall, the invaluable method we present here will advance the field of brain connectomics to a single-neuron functional

projectome stage and significantly contribute to the elucidation of information processing and transmission in the brain.

References

1. Oh, S. W. *et al.* A mesoscale connectome of the mouse brain. *Nature* **508**, 207-214 (2014).
2. Han, Y. *et al.* The logic of single-cell projections from visual cortex. *Nature* **556**, 51-56 (2018).
3. Winnubst, J. *et al.* Reconstruction of 1,000 projection neurons reveals new cell types and organization of long-range connectivity in the mouse brain. *Cell* **179**, 268-281.e13 (2019).
4. Li, A. *et al.* Micro-optical sectioning tomography to obtain a high-resolution atlas of the mouse brain. *Science* **330**, 1404-1408 (2010).
5. Ragan, T. *et al.* Serial two-photon tomography for automated ex vivo mouse brain imaging. *Nat. Methods* **9**, 255-258 (2012).
6. Becker, K., Jährling, N., Saghafi, S. & Dodt, H. U. Ultramicroscopy: light-sheet-based microscopy for imaging centimeter-sized objects with micrometer resolution. *Cold Spring Harbo. Protoc.* **2013**, 704-713 (2013).
7. Lin, R. *et al.* Cell-type-specific and projection-specific brain-wide reconstruction of single neurons. *Nat. Methods* **15**, 1033-1036 (2018).
8. Cid, E. & de la Prida, L. M. Methods for single-cell recording and labeling in vivo. *J. Neurosci. Methods* **325**, 108354 (2019).
9. Cadwell, C. R. *et al.* Electrophysiological, transcriptomic and morphologic profiling of single neurons using Patch-seq. *Nat. Biotechnol* **34**, 199-203 (2016).
10. Chen, X. *et al.* High-throughput mapping of long-range neuronal projection using in situ sequencing. *Cell* **179**, 772-786.e19 (2019).
11. Gouwens, N. W. *et al.* Classification of electrophysiological and morphological neuron types in the mouse visual cortex. *Nat. Neurosci.* **22**, 1182-1195 (2019).
12. Tonegawa, S., Liu, X., Ramirez, S. & Redondo, R. Memory engram cells have come of age. *Neuron* **87**, 918-931 (2015).
13. Wang, M. *et al.* Single-neuron representation of learned complex sounds in the auditory cortex. *Nat. Commun.* **11**, 4361 (2020).
14. Li, R. *et al.* Two-photon functional imaging of the auditory cortex in behaving mice: from neural networks to single spines. *Front. Neural Circuits* **12**, 33 (2018).
15. Gong, H. *et al.* High-throughput dual-colour precision imaging for brain-wide connectome with cytoarchitectonic landmarks at the cellular level. *Nat. Commun.* **7**, 12142 (2016).
16. Rothschild, G., Nelken, I. & Mizrahi, A. Functional organization and population dynamics in the mouse primary auditory cortex. *Nat. Neurosci.* **13**, 353-360 (2010).

17. Judkewitz, B., Rizzi, M., Kitamura, K. & Häusser, M. Targeted single-cell electroporation of mammalian neurons in vivo. *Nat. Protoc.* **4**, 862-869 (2009).
18. Quan, T. *et al.* NeuroGPS-Tree: automatic reconstruction of large-scale neuronal populations with dense neurites. *Nat. Methods* **13**, 51-54 (2016).
19. Ohno, S. *et al.* A morphological analysis of thalamocortical axon fibers of rat posterior thalamic nuclei: a single neuron tracing study with viral vectors. *Cereb. Cortex* **22**, 2840-2857 (2012).
20. Packer, A. M., Russell, L. E., Dalgleish, H. W. & Häusser, M. Simultaneous all-optical manipulation and recording of neural circuit activity with cellular resolution in vivo. *Nat. Methods* **12**, 140-146 (2015).

Methods

Animals. All experimental procedures related to the use of animals were approved by the Third Military Medical University Animal Care and Use Committee and were carried out in accordance with institutional animal welfare guidelines. Adult (8-12 weeks old) male C57BL/6J mice were obtained from the Laboratory Animal Center at the Third Military Medical University. The mice had food and water *ad libitum*, and they were housed in a humidity- and temperature-controlled room with a 12 h light/dark (lights off at 19:00) cycle.

Auditory stimulation. Auditory stimuli were delivered through a free-field ES1 speaker using an ED1 electrostatic speaker driver (Tucker Davis Technologies). The speaker was placed ~6 cm from the mouse ear, which is contralateral to the recorded A1[21-23]. The auditory stimuli were generated by a custom LabVIEW 2016 program (National Instruments) and converted to analogue voltages with a PCI6731 card (National Instruments). A pre-polarized condenser microphone (377A01 microphone, PCB Piezotronics Inc.) was used to calibrate the generated sounds. In order to establish the FRA of each neuron, sequences of pure tones (50 ms duration) consisting of 5 sound levels (30–80 dB sound pressure level (SPL), 10 dB attenuation) and 11 frequencies (logarithmic scale from 2 to 40 kHz) were presented with 8 repetitions and randomized intervals of 2-4 s. During auditory stimulation, no other sensory stimulus was present to the mouse.

Two-photon Ca^{2+} imaging in the mouse auditory cortex. A custom-built two-photon microscope (LotosScan 1.0, Suzhou Institute of Biomedical Engineering and Technology, Chinese Academy of Sciences, China)[24] was used to perform two-photon Ca^{2+} imaging experiments. Excitation light of 920 nm wavelength was delivered to the brain with a Ti:Sa laser (power of 30-120 mW, mode locked, “Mai-Tai DeepSee”, Spectra Physics) and a water-immersion objective (40×, 0.8 NA, Nikon Corporation). I Two-photon images (600 pixels × 600 pixels) were recorded at a 40 Hz frame rate.

To conduct Ca^{2+} imaging in awake mice[14], we habituated the mouse to head fixation with a titanium head post and exposed the right primary auditory cortex under isoflurane anaesthesia. A custom-made recording chamber was attached to the skull with cyanoacrylate glue (UHU). A craniotomy (~2 mm × 2 mm) was performed above A1 (location centre: bregma -3.0 mm, 4.5 mm lateral to midline), with filling

with 1.5% low-melting-point agarose. The recording chamber was perfused with normal artificial cerebral spinal fluid (ACSF) containing (in mM) 125 NaCl, 4.5 KCl, 26 $NaHCO_3$, 1.25 NaH_2PO_4, 2 $CaCl_2$, 1 $MgCl_2$ and 20 glucose, and the pH was 7.4 when equilibrated with 95% oxygen and 5% CO_2. To perform bolus loading, Cal-520 AM[25] at a concentration of 567 μM was obtained by dissolving it in DMSO with 20% Pluronic F-127. A puller (PC-10; Narishige, Tokyo, Japan) was used to make a glass pipette, with setting the pulling mode as two-stage and a heavy type. The electrode was filled with normal ACSF, and its tip maintained a resistance of 2 MΩ. The glass electrode was controlled to approach the area of interest with a pressure of 30 mbar and to inject dye solution with a pressure of 600 mbar (3 min). Two hours after dye injection and complete removal of isoflurane anaesthesia, Ca^{2+} imaging was performed and lasted for up to 8 h while the mouse was awake.

Data analysis for Ca^{2+} transients. We analysed the Ca^{2+} imaging data with custom-written software in MATLAB 2018b (MathWorks)[26]. Individual neurons were visually/semi-automatically identified and segmented as regions of interest (ROIs) according to cell morphology and fluorescence intensity. Fluorescence values (*f*) across time for each neuron were obtained by averaging the intensity values corresponding to the pixels within each ROI for each imaging frame. For each neuron, the baseline fluorescence f_0 was estimated as the 25th percentile of the entire fluorescence recording, and then Ca^{2+} signals were calculated as relative fluorescence changes $\Delta f/f = (f-f_0)/f_0$. Detection of Ca^{2+} transients was carried out based on an integrated thresholding approach, which was used in our previous studies[23]. The FRA of each neuron was constructed by calculating responses for the defined frequency-intensity conditions.

Two-photon-targeted plasmid electroporation and viral injection. To label a single neuron[2], a patch pipette (10–12 M resistance) containing intracellular solution and plasmid DNA (hSyn-eGFP-P2A-Cre-pA [100 ng/μl], and OGB-1-K^+ [100 μM]) was advanced towards the soma of the neuron. Then, electroporation pulses (NPI Electronic, Germany) were delivered by an MVCS-01 iontophoresis system with the following parameters: -12 V, 0.5 ms square pulses at 100 Hz for 1 s. After that, the pipette was slowly withdrawn and exchanged for electroporating another neuron. Then, AAV-dio-mGFP was locally injected near the location of the electroporated neurons (~300 mbar, 2 min) by a glass pipette (resistance 2 MΩ)[2]. Two coverslips, a small coverslip with a 1.5 mm diameter positioned below and a large coverslip with a 2.5 mm diameter positioned above, were used to cover the brain and part of the skull, respectively. Afterwards, dental acrylic and ultraviolet cured optical adhesives (Norland Products Inc., USA) were used to seal the skull.

Retrograde tracing. To label the contralateral auditory cortex-projecting neurons that are located in the auditory cortex, we injected viral solution (AAV2/2-Retro-hSyn-H2B-mRuby3-WPRE-pA) into the contralateral auditory cortex with a patch pipette (resistance 2 MΩ)[2]. The viral solution was loaded by applying pressure (~300 mbar, 2 min) to the glass. Fourteen days after viral injection, the labelled neuronal somata were observed in the auditory cortex by two-photon imaging *in vivo*. A subgroup of the labelled auditory neurons was chosen for electroporation, as shown in Fig. 2.

Plasmid and AAVs. The plasmid used in this study was Cre-GFP (hSyn-eGFP-P2A-Cre-pA, 100 ng/μl) for single-cell electroporation. The plasmid was purchased from Genscript Co., Ltd. (Nanjing, China). The AAVs used in this study were AAV-hSyn-dio-mGFP (AAV2/9, titer: 2.59× 10^{12} viral particles/mL) and AAV-Retro-hSyn-H2B-mRuby3-WPRE-pA (AAV2/2, titer: 2.59× 10^{12} viral particles/mL). All AAVs used in our experiments were obtained from Taitool Bioscience Co., Ltd. (Shanghai, China).

fMOST imaging. In brief, brain samples were first dissected and post-fixed in 4% paraformaldehyde at 4 °C for 24 h and then rinsed with 0.01 M PBS (Sigma-Aldrich) and embedded in Lowicryl HM20 (Electron Microscopy Sciences) before the imaging experiment. Afterwards, the resin-embedded brains were transferred to an fMOST system (BioMapping5000, Wuhan OE-Bio Co.,Ltd.)[27,28] with an imaging resolution of 0.3 × 0.3 × 1 μm^3 and imaged in a water bath filled with PI. The entire brain sample was imaged in the coronal plane for both the GFP and PI channels and then sliced to 1 μm or 2 μm via a diamond knife. The cycle of brain imaging and sample sectioning was continuously conducted until finishing the data acquisition step[29]. To improve the signal-to-noise ratio of the fMOST imaging data recorded from both the GFP and PI channels, image preprocessing procedures, including image stitching, brightness adjustment and noise filtering, were then carried out. The preprocessed imaging data were saved for both the PI and GFP channels.

Single-cell reconstruction. We transformed the preprocessed data platform to cuboid data via TDat software[30]. After importing the data into Amira software (version 6.1.1, FEI), we viewed the image stacks and traced the neurite skeletons in an interactive manner using the filament editor[7]. Two experienced annotators traced each neuron independently and then compared their reconstructions to produce a final consensus. All traced points for reconstructing neurons were saved in SWC format.

Image registration and quantitative analysis. The whole-brain imaging data were registered to a 3D reference brain atlas called the Allen Common Coordinate Framework (CCF)[31]. The imaging data recorded from the PI channel were downsampled to a spatial resolution of 10 × 10 × 10 μm^3. First, imaged brains were corrected with rigid registration. A greyscale-based 3D affine registration was used for aligning to the Allen Brain Atlas, followed by using dense landmark-based 2D registration in local regions. All registration processes were performed using Elastix[32]. Subsequently, the traced points of neuron reconstructions were transformed into Allen Brain Atlas space using the parameters for the registration transformation. Two experienced analysts checked the image registration results by back-to-back manual confirmation. Quantitative analyses of morphological features were performed using Amira and custom-written software in MATLAB. Branch lengths for both axons and dendrites were measured by summing the distances from the traced points to their parent nodes. Branch numbers for both axons and dendrites were measured by counting segments that connect to their parent nodes.

Reporting summary. Further information on the research design is available in the Nature Research Reporting Summary linked to this article.

Data availability

The data that support the findings of this study are available from the corresponding author upon reasonable request.

Code availability

The code supporting the current study has not been deposited in a public repository, but it is available from the corresponding author upon request.

References

21. Chen, X., Leischner, U., Rochefort, N. L., Nelken, I. & Konnerth, A. Functional mapping of single spines in cortical neurons in vivo. *Nature* **475**, 501-505 (2011).
22. Li, J. *et al.* Functional imaging of neuronal activity of auditory cortex by using Cal-520 in anesthetized and awake mice. *Biomed. Opt. Express* **8**, 2599-2610 (2017).
23. Li, J. *et al.* Primary auditory cortex is required for anticipatory motor response. *Cereb. Cortex* **27**, 3254-3271 (2017).
24. Jia, H., Varga, Z., Sakmann, B. & Konnerth, A. Linear integration of spine Ca2+ signals in layer 4 cortical neurons in vivo. *Proc. Natl. Acad. Sci. U.S.A.* **111**, 9277-9282 (2014).
25. Tada, M., Takeuchi, A., Hashizume, M., Kitamura, K. & Kano, M. A highly sensitive fluorescent indicator dye for calcium imaging of neural activity in vitro and in vivo. *Eur. J. Neurosci.* **39**, 1720-1728 (2014).
26. Guan, J. *et al.* NeuroSeg: automated cell detection and segmentation for in vivo two-photon Ca(2+) imaging data. *Brain Struct. & Funct.* **223**, 519-533 (2018).
27. Wang, X. *et al.* Genetic single neuron anatomy reveals fine granularity of cortical axo-axonic cells. *Cell Rep.* **26**, 3145-3159.e5 (2019).
28. Wang, X. *et al.* Chemical sectioning fluorescence tomography: high-throughput, high-contrast, multicolor, whole-brain imaging at subcellular resolution. *SSRN*, 1-50, doi:10.2139/ssrn.3677215 (2020).
29. Gong, H. *et al.* Continuously tracing brain-wide long-distance axonal projections in mice at a one-micron voxel resolution. *NeuroImage* **74**, 87-98 (2013).
30. Li, Y. *et al.* TDat: An efficient platform for processing petabyte-scale whole-brain volumetric images. *Front. Neural Circuits* **11**, 51 (2017).
31. Wang, Q. *et al.* The allen mouse brain common coordinate framework: a 3D reference atlas. *Cell* **181**, 936-953.e20 (2020).
32. 32. Klein, S., Staring, M., Murphy, K., Viergever, M. A. & Pluim, J. P. elastix: a toolbox for intensity-based medical image registration. *IEEE Trans. Med. Imaging* **29**, 196-205 (2010).

Figures

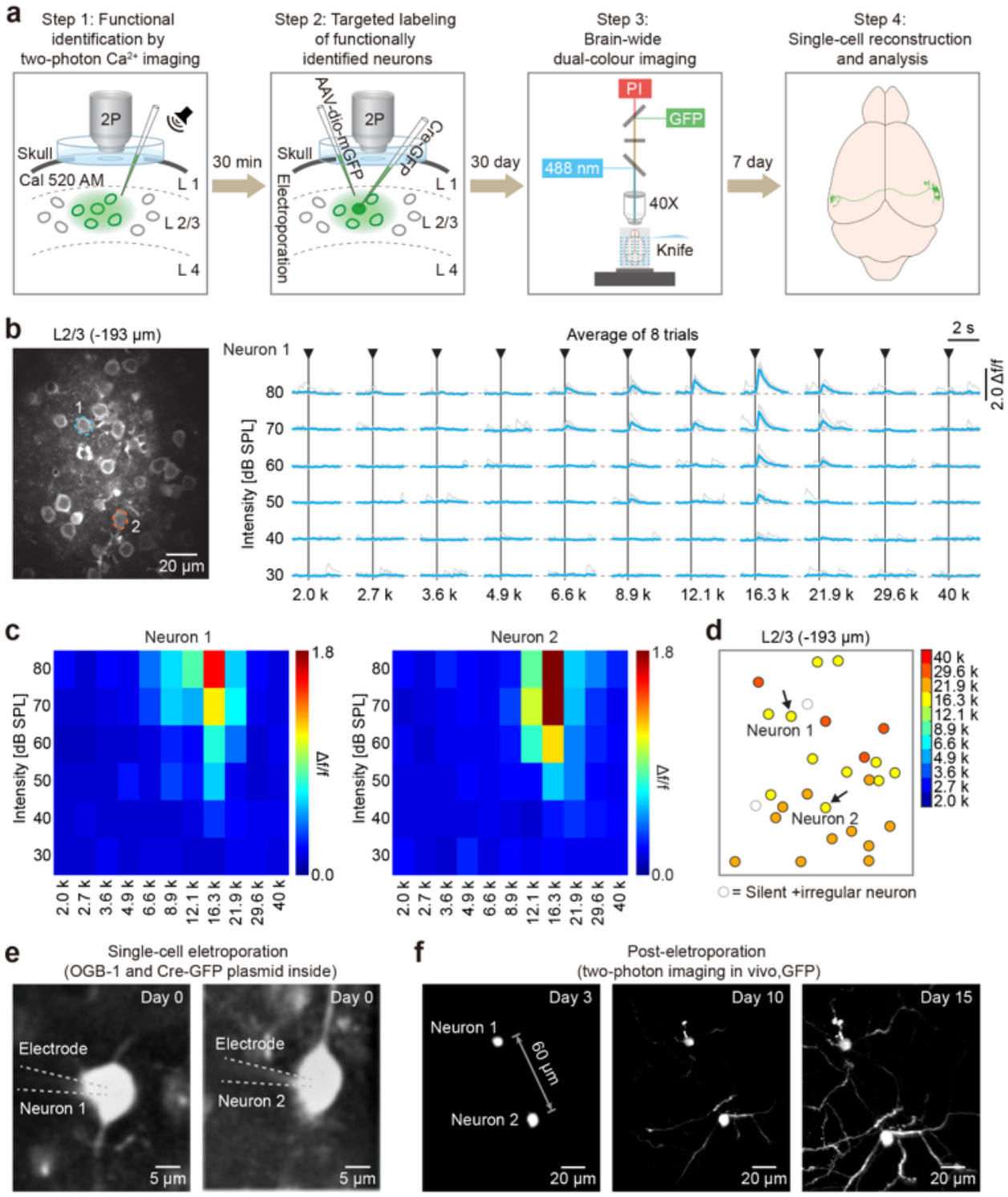

Figure 1

Online targeted labelling of single functionally defined neurons. a, Four key steps for data collection and processing. b, Left: Representative two-photon image in layer 2/3 (L2/3) of the auditory cortex of an awake mouse. Two neurons were chosen and marked with dashed coloured lines. Right: Ca2+ transients (neuron 1) responding to pure-tone stimulation (average of 8 trials for each of 6 intensities and 11 frequencies). Single-trial (grey) and trial-averaged (blue) Ca2+ transients are shown. c, Colour-coded FRAs

of the two neurons marked in a. d, Best frequency map of all the neurons in the focal plane shown in a. Colour code is on the right side. e, Pipettes containing OGB-1 and Cre-GFP plasmids were advanced towards the somata of neuron 1 and neuron 2. The dye and DNA were electroporated into the neurons by applying trains of voltage pulses. f, Monitoring the fluorescence intensities of the two electroporated neurons by two-photon imaging on different days (day 3, day 10 and day 15) after electroporation.

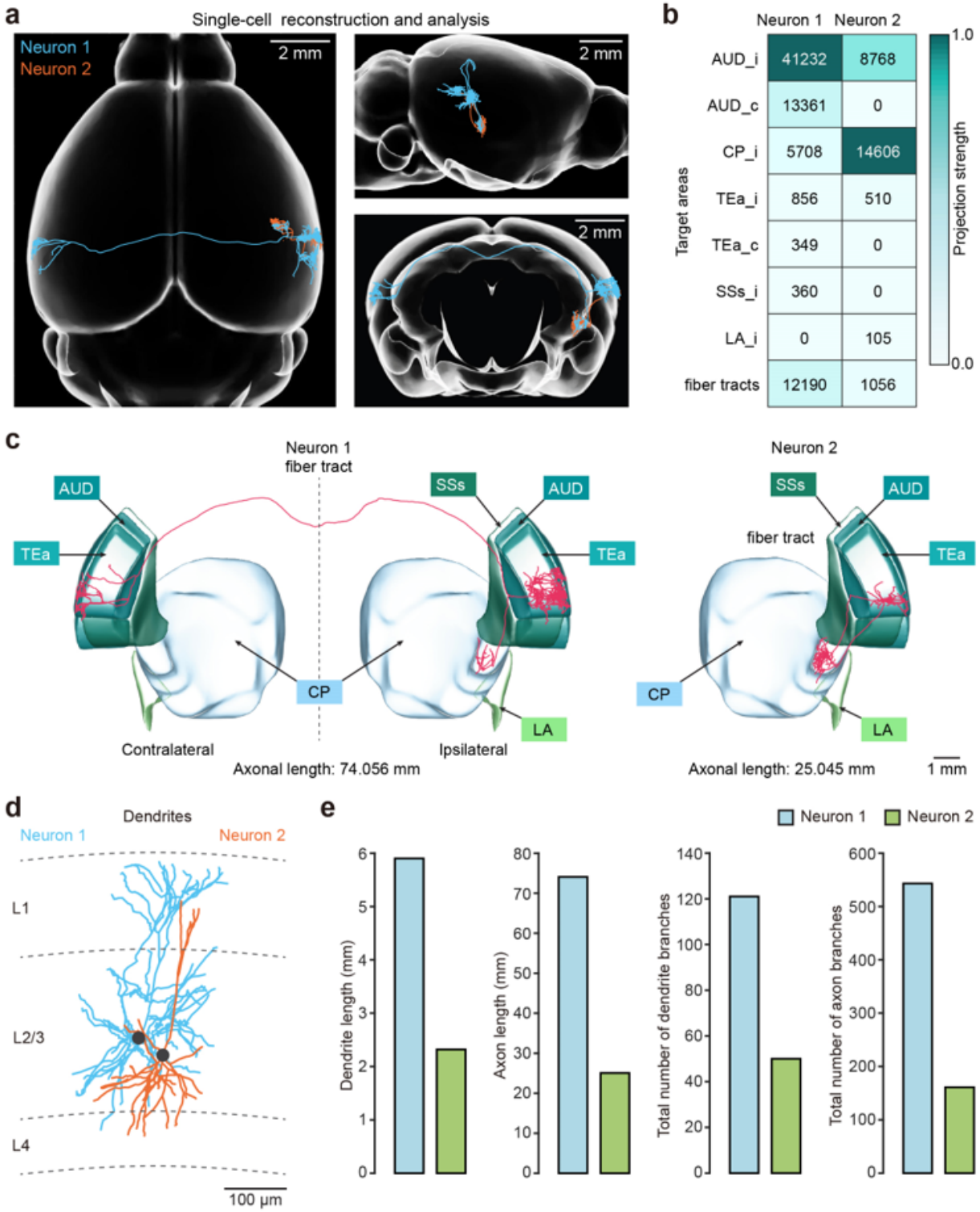

Figure 2

Whole-brain reconstruction of single functionally defined neurons. a, The two electroporated neurons were aligned to the Allen Brain Atlas. Three different views are shown (horizontal, sagittal, and coronal). b, Projection patterns of the two neurons. The projection strengths of each neuron were calculated as axon length per target area normalized by the axon length for receiving the densest innervation. The colour code reflecting the projection strength is on the right side. c, The two reconstructed neurons are displayed separately. Target areas are coloured as indicated. d, The dendrites of the two reconstructed neurons. e, Comparisons of dendritic and axonal lengths, and total numbers of axonal and dendritic branches between neuron 1 and neuron 2.

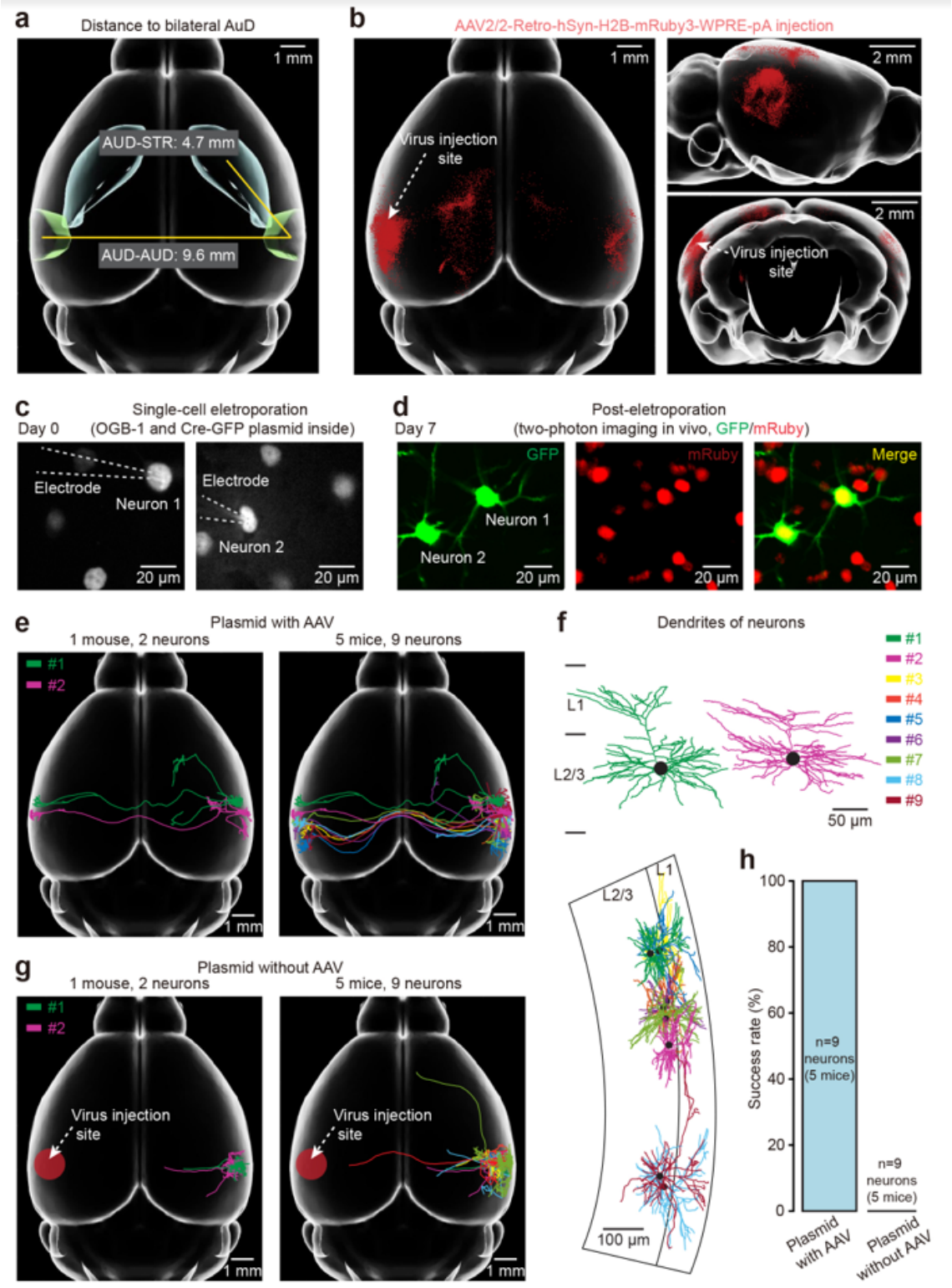

Figure 3

Axons projecting to the contralateral auditory cortex can be reliably labelled and reconstructed. a, The distance between the ipsilateral and contralateral auditory cortices is twice as long as that between the ipsilateral auditory cortex and striatum. b, The detected somata of the neurons projecting to the left auditory cortex were registered to the template of the Allen Brain Atlas. The arrow points to the AAV2/2-Retro-mRuby3 injection site in the left auditory cortex for the retrograde labelling. Three different views

are shown (horizontal, sagittal and coronal). c, Pipettes containing OGB-1 and Cre-GFP plasmid were advanced towards the somata of neurons in the right auditory cortex by applying trains of voltage pulses for electroporation. d, Monitoring the fluorescence intensities of the two electroporated neurons by two-photon imaging on day 7 after electroporation. e, Left, reconstruction of two representative neurons labelled by plasmid together with local nearby AAV injection, obtained from one brain. Right, reconstruction of nine neurons labelled by plasmid with local nearby AAV injection, obtained from 5 brains. f, The reconstructed dendrites of the two representative neurons (top) and nine neurons (bottom). g, Left, reconstruction of two representative neurons labelled by plasmid without nearby AAV injection in one brain. Right, reconstruction of 9 neurons labelled by plasmid without nearby AAV injection from 5 brains. h, Comparison between the success rates of filling axonal termination in the contralateral auditory cortex by plasmid with AAV injection and without AAV injection (5 mice for each group).

Supplementary Files

This is a list of supplementary files associated with this preprint. Click to download.

- SupplementaryInformation.docx
- SupplementaryVideo1.mov
- SupplementaryVideo2.mov